# X-BAND TRISECTION SUBSTRATE-INTEGRATED WAVEGUIDE QUASI-ELLIPTIC FILTER

**A. Ismail, M. S. Razalli[†], M. A. Mahdi, R. S. A. R. Abdullah
N. K. Noordin and M. F. A. Rasid**

Department of Computer and Communication Systems Engineering
Faculty of Engineering
Universiti Putra Malaysia
Serdang, Malaysia

**Abstract**—A narrowband trisection substrate-integrated waveguide elliptic filter with coplanar waveguide (CPW) input and output ports is proposed and demonstrated for X-band applications. The filter is formed by incorporating metallized vias in a substrate (RT/Duroid) to create cross-coupled waveguide resonators. The result is an attenuation pole of finite frequency on the high side of the passband, therefore exhibiting asymmetric frequency response. The fabricated trisection filter with a centre frequency of 10.05 GHz exhibits an insertion loss of 3.16 dB for 3% bandwidth and a return loss of −20 dB. The rejection is larger than 15 dB at 10.37 GHz.

## 1. INTRODUCTION

There is an increasing demand and interest in a variety of applications for microwave filters. In the millimeter-wave region, distributed element microwave circuits always demand low loss transmission lines. Planar forms of transmission line such as coplanar waveguide (CPW) have become one of the most widely used transmission lines in monolithic microwave integrated circuits (MMICs) due to the simplicity of fabrication and its ability to easily integrate series and shunt elements [1–3, 11]. Rectangular waveguides still play an important role [9, 10, 12–14], especially in very high frequency systems, where the loss in such a waveguide is significantly less than that in a popular planar transmission lines. For distributed element filters,

[†] Also with School of Computer and Communication Engineering, Universiti Malaysia Perlis, Perlis, Malaysia

CPW is seldom used in the millimeter-wave range due to its large insertion loss. Since CPW and rectangular waveguide together play an important role as microwave devices, effective transitions between the two are required in practical systems. In this paper, we discuss a substrate-integrated waveguide introduced in [3, 15] together with a transition from waveguide to CPW. A filter with a single transmission null is discussed for RF/microwave applications that require the higher selectivity of deep nulls on either the high side or the low side of the passband [4, 16–18]. This type of response can be obtained by a trisection filter.

The low loss rectangular waveguide-like trisection filter maintains a basically planar structure, and has high selectivity on one side of the passband.

## 2. TRISECTION SUBSTRATE-INTEGRATED WAVEGUIDE CROSS COUPLED FILTER

Figure 1 shows the basic structure of the proposed elliptic bandpass filter. The filter is composed of three substrate-integrated waveguide resonators. The resonators are formed by incorporating vias to create sidewalls inside a piece of dielectric substrate with top and bottom metallization. The substrate-integrated waveguide cavity resonator operates similarly to conventional rectangular cavity resonator. The $i$th and $j$th resonators are coupled by using wider spacing of vias between them, thus creating a window denoted by $lkc_{ij}$ as shown in Fig. 1.



(a)                                                  (b)
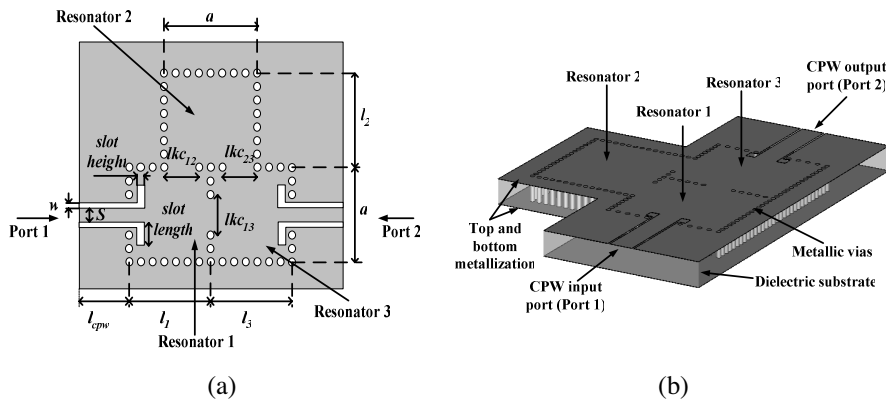
**Figure 1.** Trisection substrate-integrated waveguide elliptic filter with CPW input and output ports, (a) Top view, (b) Perspective view.

Preliminary to the filter design, analysis on radiation loss contributed by the centre-to-centre spacing ($s_c$) between adjacent vias of the substrate-integrated waveguide was simulated using [7], with substrate air in an open boundary. The dielectric and conductor losses are not considered in the simulations; therefore the loss solely comes from the radiation. The influence of $s_c$ on the loss with diameter of via ($d$) as the parameter is shown in Fig. 2. The values are normalized by the minimum guide wavelength within the bandwidth.
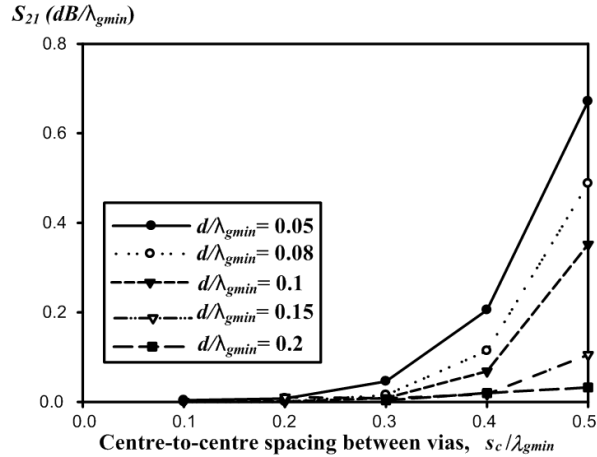


**Figure 2.** Plot of $S_{21}$ as a function of the centre-to-centre spacing between the vias for various values of the diameter of the vias. Both $s_c$ and $d$ are normalized with respect to the minimum wavelength within the bandwidth.

These curves indicate that $s_c$ must be kept small to reduce the loss between adjacent vias, suggesting that $s_c$ should be less than $\lambda_{g\,min}/2$ in order to achieve small insertion loss of less than 0.5 dB per wavelength over the frequency band. Ideally, to obtain a good performance, it is suggested from Fig. 2 that the number of vias are 10 per wavelength. However, the diameter of the vias also affects the loss and as a result, the ratio $d/s_c$ must also be considered. This is so because the diameter of vias and the spacing between the vias are interrelated. For $d < 0.2\lambda_{g\,min}$, the radiation loss is lower than 0.03208 dB/wavelength with a ratio $d/s_c$ of 0.5. The loss tends to decrease, as the diameter of via gets smaller for a constant ratio of $d/s_c$. Therefore, in this filter design, in order to achieve negligible radiation loss between adjacent vias, the diameter of the vias used is 0.6 mm with the average ratio of $d/s_c$ kept below 0.5 and $s_c$ less than $\lambda_{g\,min}/2$.

The input and output are coupled through CPW. Due to their proximity, the cross coupling between resonators 1 and 3 exists. A narrowband three-pole trisection filter has the equivalent circuit [5] shown in Fig. 3. The mutual inductance or coupling coefficient $M_{ij}$ refers to the $i$th and $j$th resonator.
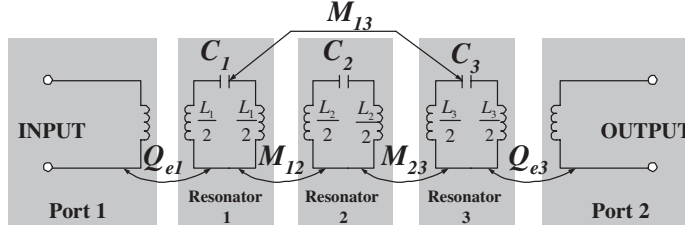


**Figure 3.** Equivalent circuit of a three-pole trisection filter [5].

The cross coupling, $M_{13}$ will determine the selectivity at a finite frequency. The external quality factors are denoted by $Q_{e1}$ and $Q_{e3}$ at the input and output ports. A trisection filter will have an attenuation pole at one side of the passband, and it requires the resonators to be asynchronously tuned to give an asymmetric filter frequency response. Thus, the resonating frequency for each resonator may be different and must be chosen to satisfy the filter requirements.

The angular resonant frequency of resonator $i$ is given by [5]

$$\omega_{0i} = \frac{1}{\sqrt{L_i C_i}} = 2\pi f_{0i} \quad \text{for} \quad i = 1, 2, 3 \tag{1}$$

where $L_i$ and $C_i$ are the inductance and capacitance values of the equivalent circuit.

To keep the physical configuration of the filter symmetrical even though the frequency response is asymmetric, the following assumptions are made [5],

$$M_{12} = M_{23}, \tag{2}$$
$$Q_{e1} = Q_{e3} \quad \text{and} \tag{3}$$
$$\omega_{01} = \omega_{03}. \tag{4}$$

Figure 4 shows the low pass prototype filter transformed from the equivalent circuit in Fig. 3. It uses $J$ inverters with [5]

$$J_{12} = J_{23} = 1 \tag{5}$$

$J_{13}$ is the bypass inverter which represents the cross coupling. It is also true that

$$g_0 = g_4, \tag{6}$$

$$g_1 = g_3 \quad \text{and} \tag{7}$$
$$B_1 = B_3, \tag{8}$$

Here $g_i$ is the capacitance and $B_i$ is the frequency invariant susceptance of the lowpass prototype filter, while $g_0$ and $g_4$ denote the resistive terminations at the input and output ports. This is shown in Fig. 4.
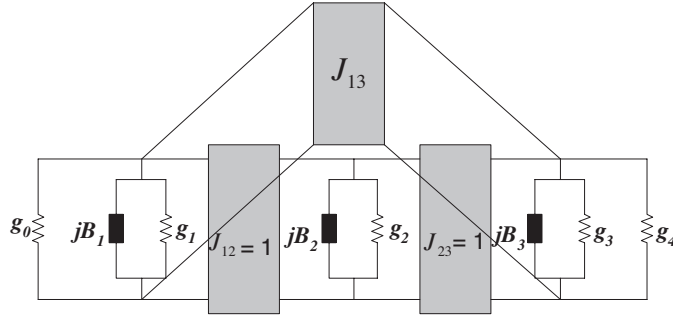


**Figure 4.** Lowpass prototype filter using admittance ($J$) inverter for three-pole trisection filter [2].

The unknown low pass element values may be determined by a synthesis method [6] or through an optimization process. Once they are determined, the circuit parameters in Fig. 3 can be found by [5]

$$Q_{e1} = \frac{b_1}{g_0} = \frac{\omega_{0i}}{\omega_0 g_0} \left( \frac{g_1}{FBW} + \frac{B_1}{2} \right), \tag{9}$$

$$Q_{en} = \frac{b_n}{g_{n+1}} = \frac{\omega_{0n}}{\omega_0 g_{n+1}} \left( \frac{g_n}{FBW} + \frac{B_n}{2} \right) \quad \text{and} \tag{10}$$

$$M_{ij}|_{i \neq j} = \frac{J_{ij}}{\sqrt{b_i b_j}} = \frac{\omega_0}{\omega_{0i} \omega_{0j}} \frac{FBW J_{ij}}{\sqrt{\left( g_i + FBW \frac{B_i}{2} \right) \left( g_j + FBW \frac{B_j}{2} \right)}}. \tag{11}$$

where $n$ is the order of the filter.

If the cross coupling is positive, i.e., $M_{13} > 0$ or $J_{13} > 0$, the attenuation pole of finite frequency is on the high frequency side of the passband, whereas if the cross coupling is negative, i.e., $M_{13} < 0$ or $J_{13} < 0$, the attenuation pole of finite frequency is on the low side of the passband. We demonstrate that the filter configuration in Fig. 1 has an attenuation pole of finite frequency above the passband owing to the cross coupling of resonators 1 and 3.

## 3. DESIGN OF SUBSTRATE-INTEGRATED WAVEGUIDE FILTER WITH CPW INPUT AND OUTPUT PORTS

For our demonstration, the filter is designed to meet the following specifications; centre frequency $= 10$ GHz, bandwidth of passband $= 0.3$ GHz (fractional bandwidth of 3%), return loss in the passband $\leq -20$ dB and rejection $> 20$ dB for frequencies $\geq 10.32$ GHz. The element values of the low pas prototype [8] filter are found to be $g_1 = g_3 = 0.68334$, $g_2 = 1.38933$, $B_1 = B_3 = 0.131$, $B_2 = -0.89316$, $J_{12} = J_{23} = 1.0$, $J_{13} = -0.51059$.

Having obtained the element values [8], the design parameters for the X-band trisection filter are calculated as follows [8]:

Resonant frequency for resonator 1 and 3;

$f_{01} = f_{03} = 9.971$ GHz,

Resonant frequency for resonator 2;

$f_{02} = 10.0969$ GHz,

External quality factor;

$Q_{e1} = Q_{e3} = 22.778$,

Coupling coefficient for resonator 1, 2 and 3;

$M_{12} = M_{23} = 0.030792$, $M_{13} = -0.022416$.

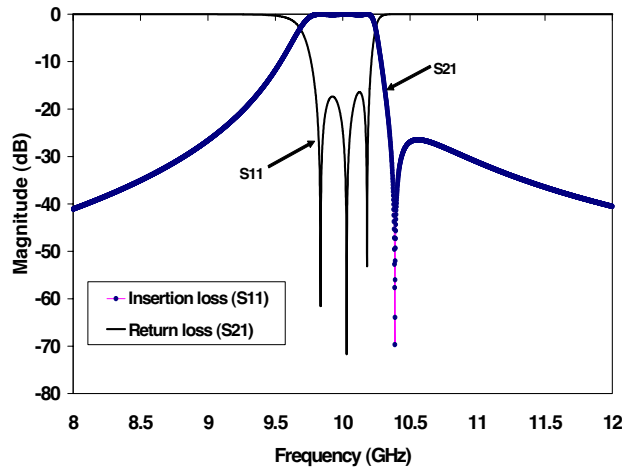Shown in Fig. 5 is the theoretical frequency response of the filter.



**Figure 5.** Theoretical response of the substrate-integrated waveguide trisection filter with an attenuation pole on the high side of the passband.

The dimension of the transition determines the external quality factor. The external quality factor $Q_e$ for resonator 1 and 3 is calculated by using a 3-D electromagnetic simulator [7] using the model shown in Fig. 6.
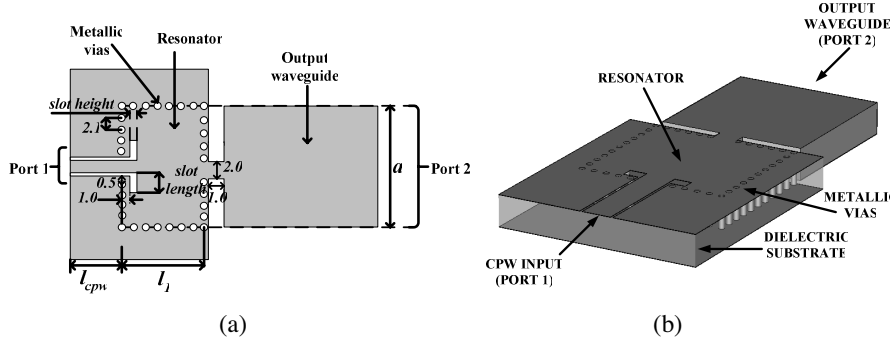


**Figure 6.** Extracting $Q_e$ for the X-band via waveguide trisection filter, (a) Top view, (b) Perspective view ($a = 15\,\text{mm}$, $l_{cpw} = 10\,\text{mm}$).

The $Q_e$ is controlled by changing the slot length of the CPW-to-waveguide transition. $Q_e$ is obtained from the simulation by [5]

$$Q_e = \frac{f_0}{f_{-3\,\text{dB}}} \tag{12}$$

where $f_0$ is the resonant frequency of the resonator and $f_{-3\,\text{dB}}$ is the 3 dB bandwidth centre at the resonant frequency.

Figure 7 shows the simulated $Q_e$ with a resonant frequency of 10 GHz. The $Q_e$ gradually decreases as the slot length becomes large. According to Fig. 7, as required for the filter specification, $Q_{e1} = Q_{e3} = 22.78$ is obtained at *slot length* $= 1.72\,\text{mm}$. Fig. 8 and Fig. 9 show the model to calculate the cross coupling between resonator 1 and 3, and the coupling between adjacent resonators 1 and 2, respectively.

The length of the window $lkc_{ij}$ as depicted in Fig. 8 and Fig. 9 controls the degree of coupling between two resonators. The length $l_1$ and $l_3$ in Fig. 8 for resonator 1 and 3 are tuned so that it has a resonant frequency of 9.97 GHz as calculated in (1).

To extract the coupling coefficient between adjacent resonators ($M_{12} = M_{23}$) in Fig. 9, resonator 1 and 2 is asynchronously tuned to each individual resonant frequency. For resonator 2, $l_2$ is optimized to give a resonating frequency of 10.09 GHz.

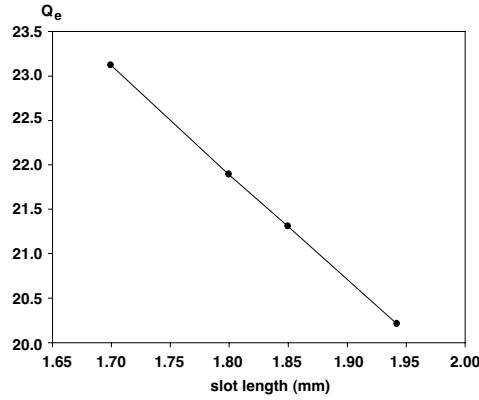The coupling coefficient $M_{12}$ can be calculated using (13) for

**Figure 7.** $Q_e$ with variation of *slot length* for the narrowband X-band substrate-integrated waveguide trisection filter.
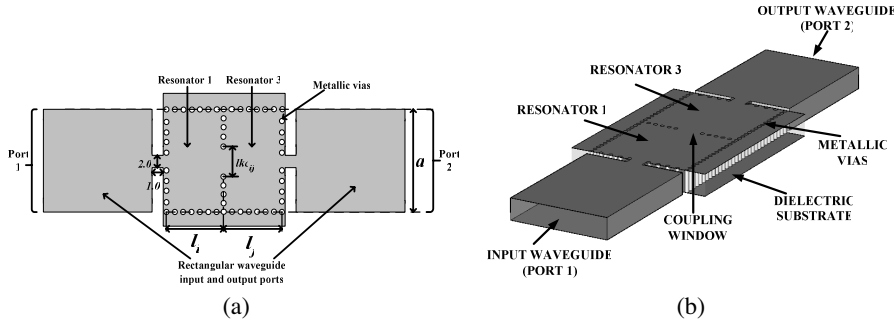


**Figure 8.** Plane view of the model to calculate the coupling coefficient, $M_{13}$ for resonator 1 and 3, (a) Top view, (b) Model used in the simulator.

asynchronously tuned coupled resonators [5]

$$k_{ij} = \frac{1}{2}\left(\frac{f_{02}}{f_{01}} + \frac{f_{01}}{f_{02}}\right)\sqrt{\frac{f_2^2 - f_1^2}{f_2^2 + f_1^2} - \left(\frac{f_{02}^2 - f_{01}^2}{f_{02}^2 + f_{01}^2}\right)} \qquad (13)$$

where $f_{01}$ and $f_{02}$ is the resonating frequency for the $i$th and $j$th resonator respectively with $f_1$ and $f_2$ are the two frequency peaks. Since resonator 1 and 3 is synchronously tuned to have the same resonant frequency, the cross coupling coefficient between the two resonators, namely $M_{13}$ in Fig. 8 can be calculated using (14) [5].

$$k_{ij} = \frac{f_e^2 - f_m^2}{f_e^2 + f_m^2} \qquad (14)$$

where $f_e$ and $f_m$ are two resonant frequencies with perfect electric and magnetic planes at the center.

    Figure 10 shows the coupling coefficients $M_{ij}$ with various values of $lkc_{ij}$, obtained using an electromagnetic CAD simulator [7]. The larger coupling is obtained for the larger spacing $lkc_{ij}$. According to Fig. 10(a), the coupling coefficients $M_{12} = M_{23} = 0.031$ can be obtained at $lkc_{12} = lkc_{23} = 5.4\,\text{mm}$, while the cross coupling coefficients $M_{13} = 0.022$ is obtained at $lkc_{13} = 4.09\,\text{mm}$ as required by the filter specification.
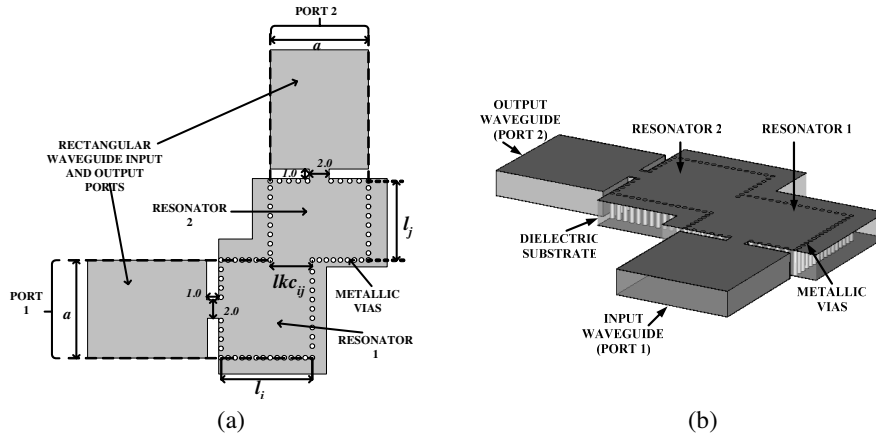


(a)                (b)

**Figure 9.** Plane view of the model to calculate the coupling coefficient $M_{12}$ for resonator 1 and 2, (a) Top view, (b) Model used in the simulator.
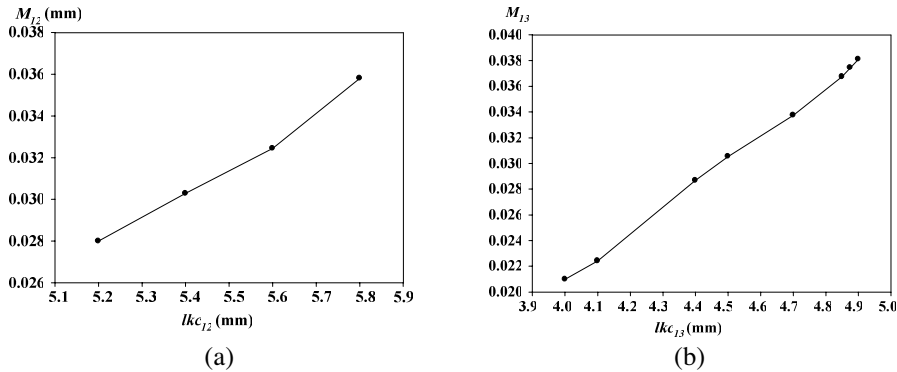


(a)                (b)

**Figure 10.** Simulated (a) coupling coefficient for resonator 1 and 2, (b) cross coupling between resonator 1 and 3.

Using the initial parameters of *slot length* and $lkc_{ij}$ obtained from the calculations above, the filter dimensions are tuned to realize the required filter response for the substrate-integrated waveguide trisection filter.

The dimensions of the X-band substrate-integrated waveguide trisection filter, according to the simulation that will satisfy the specifications are shown in Table 1. Note that the value of slot length and $lkc_{ij}$, are very close to the initial values as expected.

**Table 1.** Dimensions of an X-band substrate-integrated waveguide elliptic trisection filter.

| Parameter | Dimension (mm) |
|---|:---:|
| Width of cavity, $a$ | 15 |
| Substrate thickness, $b$ | 3.175 |
| Metal thickness, $t$ | 0.035 |
| Centre conductor of CPW, $S$ | 3.0 |
| Slot of CPW, $w$ | 0.27 |
| Length of CPW, $l_{cpw}$ | 10 |
| Length of bent slot, *slot length* | 1.4 (Initial value = 1.72) |
| Width of bent slot, *slot height* | 1.2 |
| Length of cavity 1 and 3, $l_1 = l_3$ | 13.1 |
| Length of cavity 2, $l_2$ | 13.6 |
| Coupling window between adjacent resonators, $lkc_{12} = lkc_{23}$ | 5.7 (Initial value = 5.4) |
| Coupling window for cross coupling, $lkc_{13}$ | 4.1 (Initial value = 4.09) |

The filter has been fabricated on an RT/Duroid 5880 substrate with a relative dielectric constant, $\varepsilon_r$ of 2.2 and a thickness of 5.68 mm. SMA connectors are attached to the CPW lines at the input and output ports in order to measure the filter using a network analyzer.

The simulated and measured frequency responses of the trisection filter are shown in Fig. 11.

The simulation results have included the dielectric and conductor losses ($\tan \delta = 0.0009$ and $\sigma = 5.813 \times 10^7$ S/m). According to Fig. 11, the measured insertion loss of 3.13 dB is obtained for the trisection filter
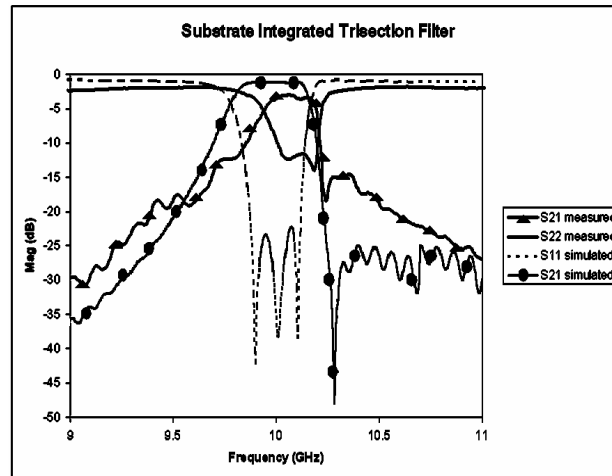
**Figure 11.** Simulated and measured frequency response for the X-band via waveguide elliptic trisection filter.

at a centre frequency of 10.09 GHz with the return loss better than $-13.5$ dB for the passband. An attenuation pole at almost exactly at 10.35 GHz is obtained, fulfilling the specification. Fabrication tolerances ($\pm 0.02$ mm), conductor loss, the tolerance in the dielectric permittivity ($\pm 0.02$) and connector mismatch have contributed to the total loss of the measured frequency responses. These are untuned results, nonetheless prove that the design method are correct and manifest the total potential in producing good agreement between simulated and measured results with proper tuning.

Even though the sidewalls of the resonators are composed of arrays of vias (or metallic posts), which involve spacings between them, the radiation loss due to the spacings are made sure to have very little effect on the overall loss performance.

## 4. CONCLUSIONS

An X-band trisection substrate-integrated waveguide elliptic filter has been designed and fabricated. The simulated frequency responses agree well with the measured. The potential of having both planar and non-planar (waveguide) circuits on a single substrate has been demonstrated with a filter with transition designs to coplanar waveguide.

Benefits for more complex microwave filters such as trisection

filters can be achieved with the proposed design of utilizing substrate-integrated waveguide in this paper.

## REFERENCES

1. Herrick, K. J., T. A. Schwartz, and L. P. B. Katehi, "Si-micromachined coplanar waveguides for use in high-frequency circuits," *IEEE Transactions on Microwave Theory and Techniques*, Vol. 46, No. 6, 762–768, June 1998.

2. Park, J.-H., C.-W. Baek, S. Jung, et al., "Novel micromachined coplanar waveguide transmission lines for application in millimetre-wave circuits," *Jpn., J. Apply. Phys.*, Vol. 39, Part 1, No. 12B, 7120–7124, December 2000.

3. Deslandes, D. and K. Wu, "Integrated transition of coplanar to rectangular waveguides," *IEEE MTT-S Digest*, 2001.

4. Hong, J.-S. and M. J. Lancaster, "Microstrip cross-coupled trisection bandpass filters with asymmetric frequency characteristics," *IEE-Proc. - Microwave Antennas Propagation*, Vol. 146, No. 1, 84–90, February 1999.

5. Hong, J.-S. and M. J. Lancaster, *Microstrip Filters for RF/Microwave Applications*, John Wiley and Sons Inc., 2001.

6. Hershtig, R., R. Levy, and K. Zaki, "Synthesis and design of cascaded trisection (CT) dielectric resonator filters," *Proceedings of European Microwave Conference*, 784–791, Jerusalem, September 1997.

7. CST Microwave Studio Version 5.3.

8. Jayyousi, A. B. and M. J. Lancaster, "A gradient-based optimization technique employing determinants for the synthesis of microwave coupled resonators," *IEEE MTT-S Digest*, Vol. 2, 1369–1372, June 2004.

9. Zhao, L.-P., X. Zhai, B. Wu, T. Su, W. Xue, and C.-H. Liang, "Novel design of dual-mode bandpass filter using rectangular structure," *Progress In Electromegnetics Research B*, Vol. 3, 131–141, 2008.

10. Ghorbaninejad, H. and M. Khalaj-Amirhosseini, "Compact bandpass filters utilizing dielectric filled waveguides," *Progress In Electromegnetics Research B*, Vol. 7, 105–115, 2008.

11. Zhang, J. and T. Y. Hsiang, "Dispersion characteristics of coplanar waveguides at subterahertz frequencies," *Journal of Electromagnetic Waves and Application*, Vol. 20, No. 10, 1411–1417, 2006.

12. He, Z. N., X. L. Wang, S. H. Han, T. Lin, and Z. Liu, "The synthesis and design for new classic dual-band waveguide band-stop filters," *Journal of Electromagnetic Waves and Application*, Vol. 22, No. 1, 119–130, 2008.

13. Khalaj-Amirhosseini, M., "Microwave filters using waveguides filled by multilayer dielectric," *Progress In Electromagnetics Research*, PIER 66, 105–110, 2006.

14. Sotoodeh, Z., B. Biglarbegian, F. H. Kashani, and H. Ameri, "A novel bandpass waveguide filter structure on SIW technology," *Progress In Electromagnetics Research Letters*, Vol. 2, 141–148, 2008.

15. Che, Q.-Q., C.-X. Li, D.-P. Wang, L. Xu, and Y. L. Chow, "Investigation on the ohmic conductor losses in substrate-integrated waveguide and equivalent rectangular waveguide," *Journal of Electromagnetic Waves and Application*, Vol. 21, No. 6, 769–780, 2007.

16. Zhang, J., J.-Z. Gu, B. Chiu, and X.-W. Sun, "Compact and harmonic suppression open-loop resonator bandpass filter with tri-section SIR," *Progress In Electromagnetics Research*, PIER 69, 93–100, 2007.

17. Mohammad Amjadi, S. and M. Soleimani, "Design of band-pass waveguide filter using frequency selective surfaces loaded with surface mount capacitors based on split-field update fdtd method," *Progress In Electromagnetics Research B*, Vol. 3, 271–281, 2008.

18. Zhang, J., B. Cui, S. Lin, and X.-W. Sun, "Sharp-rejection low-pass filter with controllable transmission zero using complementary split ring resonators (CSRRs)," *Progress In Electromagnetics Research*, PIER 69, 219–226, 2007.